Subsonic Maneuvering Effectiveness of High Performance Aircraft Which Employ Quasi-Static Shape Change Devices

Michael A. Scott[a], Raymond C. Montgomery[a], and Robert P. Weston[b]
[a]Dynamics and Control Branch, MS 132
[b]Multidisciplinary Optimization Branch, MS 159
NASA Langley Research Center
Hampton, VA 23681-0001

ABSTRACT

This paper represents an initial study on the use of quasi-static shape change devices in aircraft maneuvering. The macroscopic effects and requirements for these devices in flight control are the focus of this study. Groups of devices are postulated to replace the conventional leading-edge flap (LEF) and the all-moving wing tip (AMT) on the tailless LMTAS-ICE (Lockheed Martin Tactical Aircraft Systems - Innovative Control Effectors) configuration. The maximum quasi-static shape changes are 13.8% and 7.7% of the wing section thickness for the LEF and AMT replacement devices, respectively. A Computational Fluid Dynamics (CFD) panel code is used to determine the control effectiveness of groups of these devices. A preliminary design of a wings-leveler autopilot is presented. Initial evaluation at 0.6 Mach at 15,000 ft. altitude is made through batch simulation. Results show small disturbance stability is achieved, however, an increase in surface deflection is needed to offset five degrees of sideslip. This only applies to the specific device groups studied, encouraging future research on optimal device placement.

Keywords: SMA, pulsed jets, steady jets, smart structures, aircraft flight control, panel code, innovative control effectors, quasi-static shape change, control effectiveness, LMTAS-ICE, CFD.

1. INTRODUCTION

In May 1996, NASA Langley Research Center sponsored a Smart Aircraft Systems Workshop[1] to conduct a cross disciplinary review examining the feasibility of applying active structures technology to modify and control aircraft aerodynamics. The potential of controlling an aircraft using novel aerodynamic control devices was considered. These novel devices are flow control actuators (active jets, synthetic jets, active porosity devices, piezoelectric, SMA, and perhaps even others) which are expected to play a strong hand in the development of a seamless aircraft, one with no moving external control surfaces, merely hundreds or even thousands of small ports through which control of the vehicle as well as performance trimming is morphed aerodynamically. These developments may be facilitated by a new technology called MEMS (Micro-Electro-Mechanical Systems), an overview of which can be accessed via the world wide web[2].

The current state of the art in smart materials and structures falls into two general categories: quasi-static shape change (for example through SMA's) and high bandwidth actuation (such as piezoelectric and magnetostrictive materials). The quasi-static technologies are viewed as more mature. The high bandwidth actuation (using periodic excitation) has demonstrated increased lift and reduced drag at angles of incidence and flap deflections at which the flow would otherwise be separated in high Reynolds number experiments[3] ($R_c = 0.3 \times 10^6$.) The long term goals of this research are to investigate closed loop control of the quasi-static shape change and high bandwidth actuation devices using local sensing, and feedback control. For many applications, these devices will modify local phenomena to support a macroscopic strategy, such as flow separation control for advanced high lift systems. The near term focus is on quasi-static shape change devices. The goal of this paper is to conduct a preliminary assessment of quasi-static shape change devices in three-axis control of a seamless aircraft.

Further author information -
M.A.S.: Email: michael.allen.scott@larc.nasa.gov; WWW:http://dcb.larc.nasa.gov/www/DCBStaff/mas/mas.html; Telephone: 757-864-6618; Fax: 757-864-7795
R.C.M.: Email: r.c.montgomery@larc.nasa.gov; WWW:http://dcb.larc.nasa.gov/www/DCBStaff/rcm/rcm.html; Telephone: 757-864-6618; Fax: 757-864-7795
R.P.W.: Email: r.p.weston@larc.nasa.gov; WWW:http://fmad-www.larc.nasa.gov/mdob/users/weston/Personal_info/personal.html; Telephone: 757 864-2149; Fax 757-864-9713

The approach taken is to model an aircraft paper design which has a relatively high degree of definition and investigate, using computational fluid dynamics, the use of low radar cross section (RCS) quasi-static shape change devices in affecting three-axis control. The aircraft selected for study is the Innovative Control Effector aircraft studied by Lockheed Martin Tactical Aircraft Systems[4]. This aircraft is a tailless, delta-wing fighter, nearly a seamless aircraft, and thus is ideal for our purpose (Figure 1.) Low RCS design practices manifest themselves in the form of external shaping, elimination of vertical control surfaces, and alignment of control surface edges with external airframe edges. As a result, aircraft designed for low RCS require new control concepts to achieve the required maneuvering capability and tactical utility throughout the flight envelope.

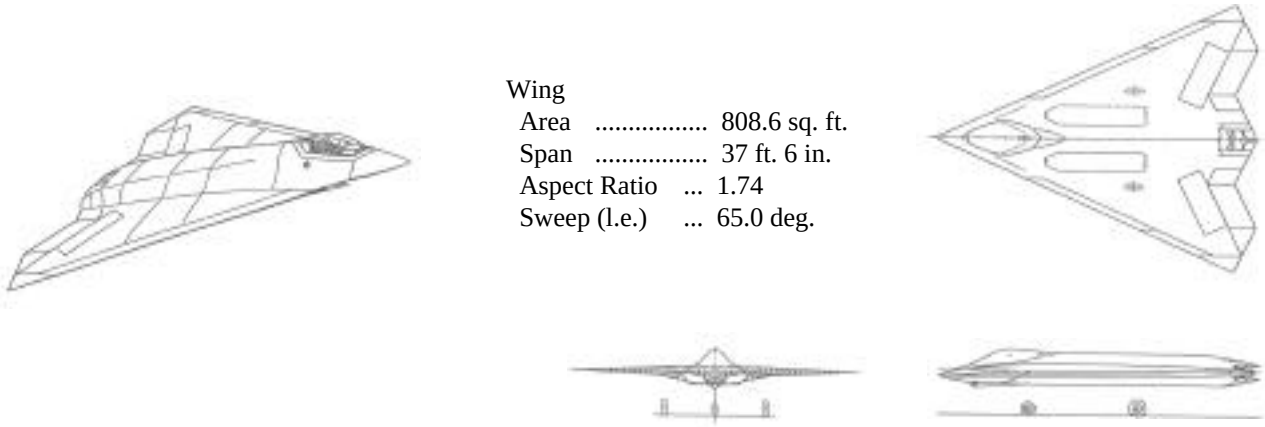

Figure 1 - ICE configuration 101

Our initial study is to examine the potential of low RCS quasi-static shape change devices to replace the all moving tips, AMT, and the leading edge flaps, LEF, which are movable surfaces. This is done for the design flight condition of a 0.6 Mach number and a 15,000 feet altitude. Low-speed, potential, CFD analysis is used to predict the effects of the quasi-static shape change on the AMT and LEF surfaces. This data is used in constructing a six degree-of-freedom simulator of the rigid body dynamics of the aircraft. This simulator is used to investigate the unaugmented aircraft dynamics. Since the longitudinal dynamics was acceptable whereas the lateral dynamics were not, the paper focuses on the design of a lateral flight control system. A wings-leveler autopilot with lateral stability augmentation system is implemented in the simulator and stabilizing feedback gains are determined through a trial and error method. This autopilot is tested in simulation in step gust inputs corresponding to a sideslip angle of 5 degrees and the size of the quasi-static shape change required are reported.

The report is organized as follows. First, the basis of the data base used, namely the computational fluid dynamics code is overviewed. Next, the modeling of the quasi-static shape change is discussed, followed directly by a presentation of the static control effectiveness studies made. Next the control system is described as well as the six degree-of-freedom dynamics simulator used for open and closed-loop dynamics studies. Finally, results of the feedback control studies are reported and suggestions are made for future research that would support technology development in this area.

2. LOW-SPEED PANEL METHODS

The basis of the computational fluid dynamics code used herein is potential theory which is briefly reviewed here. The basic theories involved have not changed since the original publication in Prandtl[5], which is a comprehensive treatment of the state of the art as it existed at that time, prior to the evolution of modern computer technology, when numerical results were few and far between. Excluding molecular flow theory, the fundamental physical equations used to obtain complete descriptions of fluid flow for aircraft are: the momentum equation; the continuity equation; the energy equation; and the state equation of the gas. Under the additional assumption of incompressibility, the continuity equation reduces to div(V)=0. With the additional assumption that the fluid is initially irrotational and inviscid, a velocity potential, Φ, exists, meaning that V = grad(Φ). The continuity equation becomes $\Delta\Phi = 0$ where

$$\Delta = \quad {}^{2} = \left(\frac{\partial^2}{\partial x^2} + \frac{\partial^2}{\partial y^2} + \frac{\partial^2}{\partial z^2}\right) \tag{1}$$

is the Laplacian operator. The solution to the flow problem is enormously simplified by the use of Green's theorem. The solution in the field can be expressed in terms of that on the boundaries, thus one need only grid the near field aircraft surface and wake boundaries. The far field boundaries are handled analytically. Most of the problems in modeling flow using this theory centers around determining boundary conditions that meet the surface geometry requirements as well as the singularities required in the flow to generate aerodynamic forces, i.e. modeling the vorticity and singular surfaces in the flow, i.e. wakes.

For potential theory, the momentum equations can be integrated analytically to yield the Bernoulli equation:

$$\frac{\partial \Phi}{\partial t} + \frac{V^2}{2} + \frac{p}{\rho} - U = f(t), \tag{2}$$

where U is the body force potential, usually $(-g \quad Lz)$. For most applications, the function $f(t)$ is zero and Eq. 2 is used to merely define pressure distributions given the time-varying solution to the potential equation $\Delta\Phi = 0$ which satisfies the boundary conditions.

Over the past several years tremendous progress has been made in solutions to fluid flow problems using potential theory, and this has led to the so-called panel methods, which incorporate far field boundary conditions analytically and the near-field boundary conditions numerically. The Green's function solution to the potential equation is:

$$\Phi(x,y,z) = \int_{\partial} \Phi(\xi,\eta,\varsigma)\mathbf{n} \quad \left(\frac{1}{r}\right) d\xi d\eta d\varsigma + \int_{\partial} \left(\frac{1}{r}\right)\mathbf{n} \quad \Phi(\xi,\eta,\varsigma) d\xi d\eta d\varsigma \tag{3}$$

where Φ satisfies Laplace's equation,

$$^2\Phi(x,y,z) = 0 \qquad (x,y,z) \qquad . \tag{4}$$

The flow velocity in is obtained from the potential solution (Eq. 3) by,

$$V(x,y,z) = \text{grad}(\Phi(x,y,z)) \ . \tag{5}$$

The Green's function solution represents the region , bounded by $\partial \quad = \left(S_{uw}, S_{lw}, S_{\infty}, S\right)$. Where $S_{uw}, S_{lw}, S_{\infty}, S$ represent the boundary conditions at the upper wake, lower wake, far field and airfoil surface respectively (Figure 2.) The far field boundary condition is given by the free stream velocity $V = (V_{\infty}, \alpha)$.

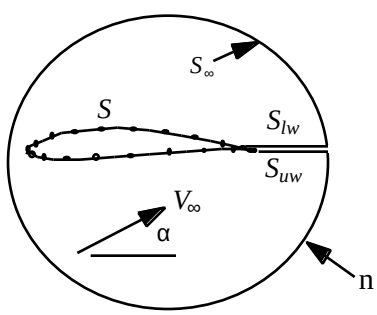

Figure 2 - Near and far field boundary condition for Greens function.

The first integrand in Eq. 3,

$$\Phi(\xi,\eta,\varsigma) d\xi d\eta d\varsigma \ , \tag{7}$$

can be thought of as a distribution of doublets, which is integrated over ∂ . The second integrand in Eq. 3,

$$\mathbf{n} \quad \Phi(\xi,\eta,\varsigma) d\xi d\eta d\varsigma \ , \tag{8}$$

is a distribution of sources, which is integrated over ∂ . The problem reduces to that of generating appropriate boundary conditions for ∂ , and then generating the distribution of sources and doublets over ∂ that meet those conditions. Panel methods do this numerically by analytically representing the boundary conditions over the far field of ∂ and discretizing the near field, i.e. breaking up the surface of an aircraft into surface elements, or panels. Katz[6] provides an excellent tutorial on these methods and a historical perspective on their development for low speed aerodynamics. The panel code used in this study, PMARC[7] (Panel Method Ames Research Center), is a production code that incorporates the nuances required for real-

time flow prediction including unsteady, time-varying flow that result from the deformation of the boundaries as well as flow through them.

3. POTENTIAL FLOW DEVICE MODELING

A surface distortion was used to model the effector device. It was felt that the surface distortion was the most general form of any device designed for mild maneuvering requiring low RCS. The validity of this assumption for SMA, piezoelectric and other real surface distortions is well justified. Other devices, such as pulsed and synthetic jets, and their effect on the flow field are less understood and are the subject of future research.

Donovan, Kral and Cary[8] performed a detailed study regarding the simulation of an isolated jet using Reynolds-averaged Navier-Stokes (RANS) equations. Their result (Figure 3) demonstrates the effect of a steady-jet on a NACA 0012 airfoil at $Re_c = 8.5 \times 10^6$ and $\alpha = 4.0°$. Shown are the streamlines for the $U_j/U_\infty = 1.0$ case. The Figure shows that the effect is to produce a distortion of the surface, as well as an effluent added to the primary flow. A proper potential model would be a surface distortion and an effluent. In this paper we assume there is zero-mass-transfer and therefor no added effluent.

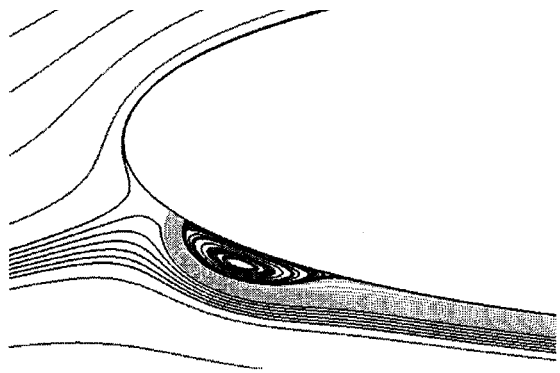

Figure 3 - Streamlines $\alpha = 4.0°$ with steady-jet control at $U_j/U_\infty = 1.0$

This initial study focused on devices that generate no net-mass-transfer. Thus, the nominal ICE configuration was modified to include quasi-static shape change, zero-mass-transfer devices. Groups of devices are postulated to replace the conventional leading-edge flap (LEF) and the all-moving wing tip (AMT) devices on the tailless, LMTAS- ICE configuration. Figure 4 is a top view of half of the ICE configuration. Shown are the locations of the shape change devices. A cross sectional view of the devices is shown in Figure 5. The maximum distortions were 13.8% and 7.7% of the section thickness for the design model LEF and AMT devices respectively.

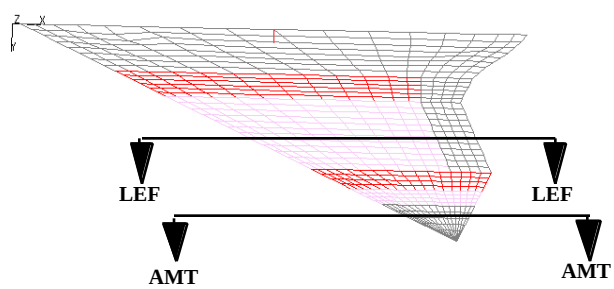

Figure 4 - LEF and AMT quasi-static shape change device section locations.

In these plots the shape change distribution is assumed to cover the leading 1/4 chord of the airfoil. For the unaugmented and augmented studies shown below, a commanded deflection of one represents a 2 inch maximum distortion for the LEF effector and a 0.25 inch deflection for the AMT effector as shown in Figure 5. A surface shape command is assumed to have the same scaled shape as shown in Figure 5. No effector optimization studies are used in this present study to select the optimal group location. The objective here is to investigate the macroscopic effect of surface changes on mild maneuvering control with very low RCS effectors. In future work, an automatic differentiation version of the PMARC code will be utilized to select optimal locations for groups of these devices.

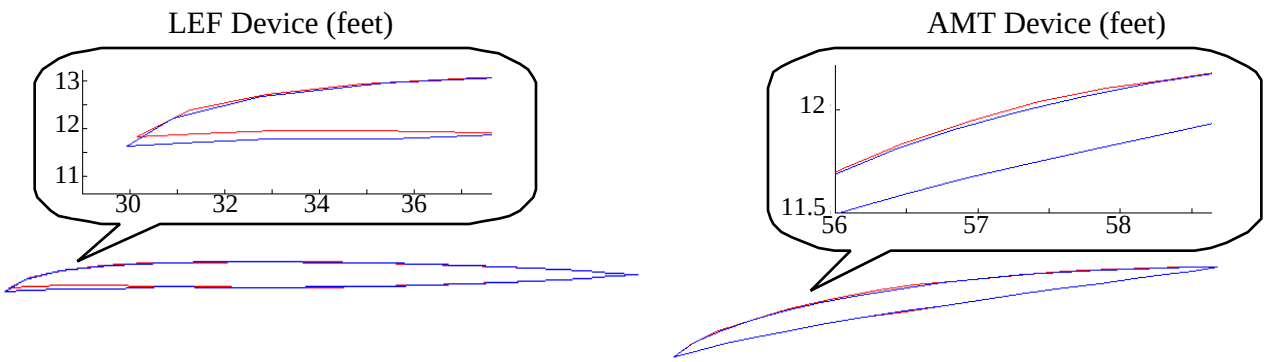

Figure 5 - LEF and AMT quasi-static shape change of the ICE-101 Configuration.

4. STATIC EFFECTIVENESS - CFD RESULTS

Static effectiveness of the surface distortions was obtained using the PMARC flow solver tool. Flight conditions for all the CFD results were $\alpha = 4.39°$ (trim alpha) and Mach = 0.6, at altitude 15000 ft. Rigid wakes were used in the PMARC flow solver using 30 panels.

Two control surfaces were investigated using the 6 geometry files listed in Table 1. The nominal configuration had no surface distortions. To decrease the computational burden, half of the geometry was used in the PMARC flow solver. These symmetric runs using PMARC generated assembly and total force and moment coefficients. The decision to use half the geometry was based on the assumption that there was little crossflow across the symmetry line of the airplane. A test case was run in PMARC to validate this assumption. These coefficients were then used to investigate the control effectiveness of the control surfaces. Figure 6 shows the axis definitions used in Table 1.

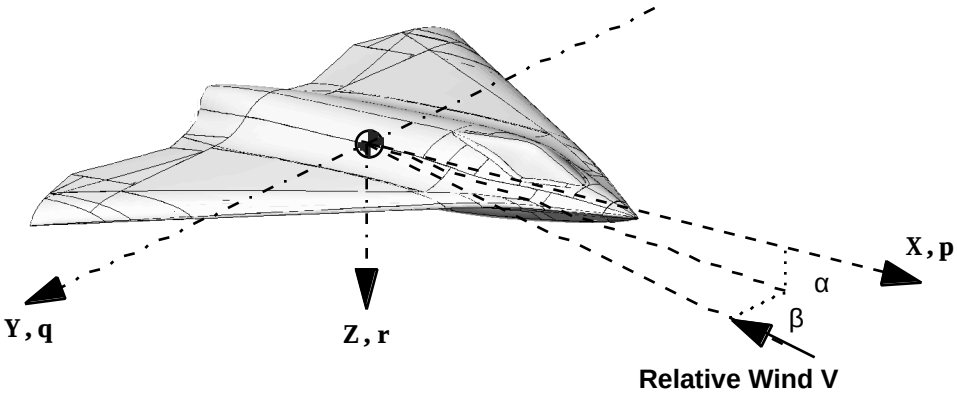

Figure 6 - ICE axis definitions.

Geometry File	Normal Force Cz	Axial Force Cx	Side Force Cy	Pitch Moment Cm	Yaw Moment Cn	Roll Moment Cl
Nominal (total)	-0.1251	0.0066	0.0000	0.0002	-0.0000	-0.0000
Nominal (one side)	-0.0625	0.0033	0.0201	0.0001	-0.0014	-0.0083
AMT (total)	-0.1258	0.0067	0.0000	-0.0004	-0.0000	-0.0000
AMT (one side)	-0.0629	0.0033	0.0202	-0.0002	-0.0015	-0.0085
LEF (total)	-0.1264	0.0067	0.0000	0.0001	-0.0000	-0.0000
LEF (one side)	-0.0632	0.0034	0.0204	0.0001	-0.0014	-0.0085

Table 1 - PMARC Results for the 6 Geometry Files.

Lateral coefficients were obtained by differencing results of the assembly coefficients of the symmetric runs for the AMT and LEF configurations with the symmetric nominal PMARC results. Thus, data in Table 1 were differenced to yield the longitudinal and lateral directional control effectiveness coefficients. In Table 2, the SAMT refers to the symmetric configuration AMT device, i.e., the AMT device is on both the right and left wing. The DAMT refers to the differential AMT device, thus the AMT is activated on the right wing only.

	Longitudinal Control			Lateral Directional Control		
Device	Axial Force Cx	Normal Force Cz	Pitch Moment Cm	Side Force Cy	Roll Moment Cl	Yaw Moment Cn
SAMT	0.0001	-0.0007	-0.0006	0	0	0
SLEF	0.0001	-0.0013	-0.0001	0	0	0
DAMT	0	-0.0004	-0.0003	0.0001	-0.0002	-0.0001
DLEF	0.0001	-0.0007	0	0.0003	-0.0002	0

Table 2 - Longitudinal and Lateral Directional Control Effectiveness Coefficients.

Only the lateral directional control coefficients were used to augment the aircraft dynamics since the ICE configuration requires no augmentation for the longitudinal motion. The maximum surface distortion on the AMT is 0.25 inches, which is 8 times smaller than the maximum surface distortion of the LEF (See Figure 5). Thus for roll maneuvers, the AMT device (on the tip of the wing) is 8 times more effective for a given surface distortion than the LEF device (on the middle of the wing). The AMT device is roughly 3 times more effective for side force for a given unit surface distortion. In this initial study, there were no optimal device location studies performed. Subsequent future studies will look at optimizing the location of the shape change using a tool called ADIFOR (Automatic Differentiation of FORTRAN - See suggestions for future research.)

5. SIX DEGREE OF FREEDOM SIMULATOR

A six degree-of-freedom dynamics simulator was used to investigate unaugmented and augmented aircraft dynamics. The representation of aerodynamics used in the simulator is a linearization of the longitudinal aerodynamic force and moment coefficients in angle of attack, α, and the quasi-static shape change effectivenesses as in the method of Bryan[9], but for the lateral coefficients, dependence on α is retained. Thus, for the longitudinal coefficients, Cx, Cz, and Cm, we take the linearization

$$Cx = Cx_o + Cx_\alpha\alpha + Cx_q q(c/2V) + Cx_{SAMT}SAMT + Cx_{SLEF}SLEF + Cx_{DAMT}DAMT + Cx_{DLEF}DLEF$$
$$Cz = Cz_o + Cz_\alpha\alpha + Cz_q q(c/2V) + Cz_{SAMT}SAMT + Cz_{SLEF}SLEF + Cz_{DAMT}DAMT + Cz_{DLEF}DLEF$$
$$Cm = Cm_o + Cm_\alpha\alpha + Cm_q q(c/2V) + Cm_{SAMT}SAMT + Cm_{SLEF}SLEF + Cm_{DAMT}DAMT + Cm_{DLEF}DLEF$$

and for the lateral coefficients, Cy, Cl, and Cn, we take

$$Cy = Cy_\beta\beta + Cy_p p(b/2V) + Cy_r r(b/2V) + Cy_{DAMT}DAMT + Cy_{DLEF}DLEF$$
$$Cl = Cl_\beta\beta + Cl_p p(b/2V) + Cl_r r(b/2V) + Cl_{DAMT}DAMT + Cl_{DLEF}DLEF$$
$$Cn = Cn_\beta\beta + Cn_p p(b/2V) + Cn_r r(b/2V) + Cn_{DAMT}DAMT + Cn_{DLEF}DLEF$$

where

$$Cy_\beta = Cy_{\beta o} + Cy_{\beta\alpha}\alpha$$
$$Cl_\beta = Cl_{\beta o} + Cl_{\beta\alpha}\alpha$$
$$Cn_\beta = Cn_{\beta o} + Cn_{\beta\alpha}\alpha$$

In the above equations

total air speed = $V = (u^2 + v^2 + w^2)^{1/2}$
angle of attack = $\alpha = \arctan(w/u)$
angle of sideslip = $\beta = \arcsin(v/V)$
dynamic pressure = qbar = $\rho \cdot V^2/2$

and c is the reference chord and b is the wing span. Also (u,v,w) and (p,q,r) are the translational and rotational rates about the body-fixed, reference (x,y,z) axes of the aircraft, respectively, and (Cx,Cy,Cz) and (Cl,Cm,Cn) are the aerodynamics force and moment coefficients about the (x,y,z) axes, respectively.

The equations of motion for the rigid body dynamics of aircraft are well developed and available in tutorial texts[10]. They require a description of the attitude of the vehicle which has traditionally been via Euler angles (ibid). These are used herein to represent the orientation of the aircraft with the sequence corresponding to ψ about the z the axis, θ about the y axis, and φ about the x axis. Thus, the kinematic differential equations implemented in the simulator are:

$$d\theta/dt = q \cdot \cos(\varphi) - r \cdot \sin(\varphi)$$
$$d\psi/dt = (q \cdot \sin(\varphi) + r \cdot \cos(\varphi))/\cos(\theta)$$
$$d\varphi/dt = d\psi/dt \cdot \sin(\theta) + p$$
$$dh/dt = u \cdot \sin(\theta) - w \cdot \cos(\theta)\cos(\varphi) - v \cdot \cos(\theta)\sin(\varphi)$$

where h is the altitude. For the longitudinal variables, the dynamic equations of motion used are:

$$du/dt = v \cdot r - w \cdot q + g((T + Cx \cdot qbar \cdot S)/W - \sin(\theta))$$
$$dw/dt = u \cdot q - v \cdot p + g(\cos(\theta)\cos(\varphi) + Cz \cdot qbar \cdot S/W)$$
$$dq/dt = (Cm \cdot qbar \cdot S \cdot c + (I_z - I_x)r \cdot p + (r^2 - p^2)I_{xz} - r \cdot H_T)/I_y$$

where g is gravity. For the lateral equations of motion, because of inertia terms, it is convenient to define the total rolling moment, L, and yawing moment, N, of the aircraft as

$$L = Cl \cdot qbar \cdot S \cdot b + (I_y - I_z) \cdot q \cdot r + p \cdot q \cdot I_{xz}$$
$$N = Cn \cdot qbar \cdot S \cdot b + (I_x - I_y) \cdot q \cdot p - q \cdot r \cdot I_{xz} + q \cdot H_T$$

where T is the engine thrust, and H_T is the moment of momentum about the x axis of the engine rotors which are assumed to be aligned with the body x axis. Assuming symmetry with respect to the x-z plane, I_x, I_y, I_z are the moments of inertia about the x,y,z axes and I_{xz} is the relevant product of inertia about the y axis. Thus, the lateral equations of motion are:

$$dv/dt = w \cdot p - u \cdot r + g(Cy \cdot qbar \cdot S/W + \cos(\theta)\sin(\varphi))$$
$$dp/dt = (I_z \cdot L + I_{xz} \cdot N)/(I_x \cdot I_z - I_{xz}^2)$$
$$dr/dt = (I_{xz} \cdot L + I_x \cdot N)/(I_x \cdot I_z - I_{xz}^2)$$

The geometry data used in the simulator are c = 28.75 ft, b = 37.5 ft, and S = 808.6 ft^2, and the mass/inertia data are W = 32750 lbf, I_x = 35479 slug-ft^2, I_y = 78451 slug-ft^2, I_z = 110627 slug-ft^2, and I_{xz} = -525 slug-ft^2. The aerodynamic coefficients not given previously are given in Tables 3-4:

	o	α	q
Cx	0.0166	-0.1973	0.
Cz	0.0395	-2.2475	0.
Cm	0.0036	-0.0467	-.39516

Table 3 - The Longitudinal Aerodynamic Coefficients for the ICE simulator.

	βo	βα	p	r
Cy	-0.0534	0.2331	0.	0.
Cl	0.0109	-0.7846	-.016	.021368
Cn	-0.0099	-0.1215	-.021789	-.01

Table 4 - The Lateral Aerodynamic Coefficients for the ICE simulator.

6. UNAUGMENTED AIRCRAFT DYNAMICS

The longitudinal dynamics for this aircraft are stable with a short period damping ratio of approximately three tenths. Thus, no longitudinal controller is therefore required for this configuration. In the lateral case, for most aircraft, including the ICE aircraft, there is no tendency to return to an initial heading and/or to correct bank angle after a disturbance from equilibrium caused by either a control surface deflection or a gust. In fact, if left unattended, many aircraft will diverge and enter into a spiral motion. Thus, the pilot must continually provide the function of a wings leveler autopilot and continually make corrections to keep the wings level and to maintain a given heading.

The unaugmented lateral directional characteristics of the aircraft are unstable as shown in Figure 7 for the simulated transient response due to a 1 degree initial bank angle. The roll rate steadily progresses to a 360 degree per second spiral in less than one minute. The yaw rate is also shown to steadily increase. This response is characteristic of an aircraft with an unstable spiral mode and a moderately stable Dutch roll mode. For an unpiloted batch simulator, these spiral dynamics produce large

excursions in attitude at low frequency which build and couple with the Dutch roll thus making it difficult to extract pertinent flight control characteristics. These large excursions are normally eliminated by a human pilot with little effort. Thus, realistic study is facilitated by using a wings leveler autopilot with a Dutch roll damper as a lateral control system. This function is essential if one is to conduct meaningful studies using a batch simulator, that is, to investigate stable operating points as if a human pilot were present. Thus, the approach taken here is to implement a wings leveler autopilot for a lateral control system.

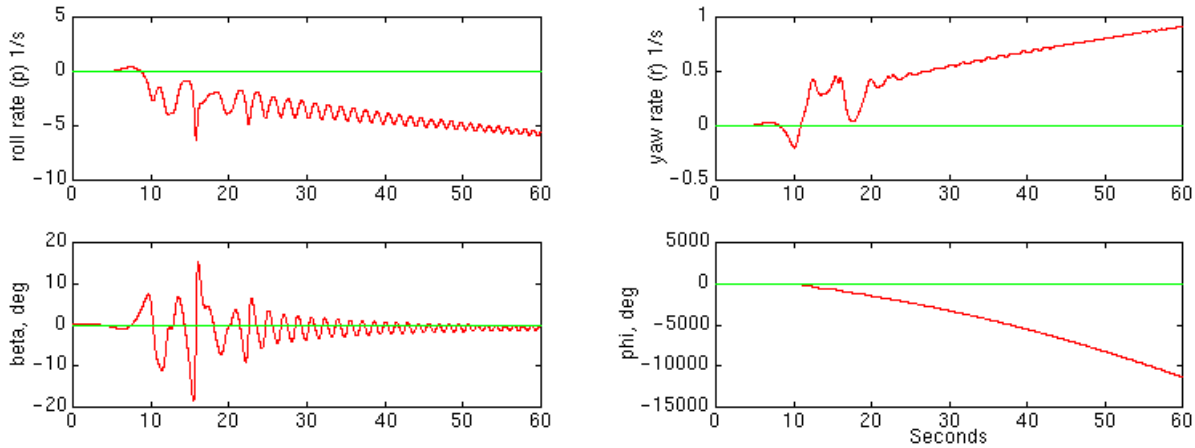

Figure 7 - Unaugmented transient response to initial bank angle.

7. WINGS LEVELER CONTROL LAW DEVELOPMENT

The wings leveler control system requires a bank angle signal which, in practice, can be derived from a vertical gyro. Also, since feedback from this attitude control loop is typically destabilizing, a Dutch roll damper may be required[11]. This can be achieved with roll and yaw rate sensors. Finally, since the vehicle has little or no directional stability, i.e. low Cn_β, the equivalent of a sideslip angle sensor may needed. In practice this can be provided by a side force accelerometer or a β-vane. Both sensors are highly undesirable but, for this study, the β-vane was assumed initially and design studies were conducted to eliminate the need for this sensor by adjusting the feedback gains on the roll and yaw rate gyros. This may be accomplished at the design flight condition, but may not be acceptable for take-off and landing since it derives the required feedback through bank excursions which may not be possible near the ground.

The fact that only a lateral autopilot is required serves to further reduce the problem since only differential control inputs are needed. So finally, the form of the autopilot required for this study is:

$$DAMT = G_{DAMT/p}p + G_{DAMT/r}r + G_{DAMT/\varphi}\varphi$$
$$DLEF = G_{DLEF/p}p - G_{DLEF/r}r + G_{DLEF/\varphi}\varphi$$

The required sensors and units of measurement used in feedback are: r (yaw rate gyro - radians/sec), p (roll rate gyro - radians/sec), and φ (bank angle - radians). The G terms in front of these sensors represent the control gain coefficients used in the control law. For this study, a trial and error, recursive method was used to select these gains based on desired dynamic responses. In future studies, linear models, extracted from the nonlinear simulation, will be used to place eigenvalues at the desired locations in a closed form solution. The control logic which drives SAMT, SLEF, DAMT, and DLEF is simulated as a zero-order-hold, sampled data system. For this study the sample frequency is 100 samples per second.

The design process was to first select a feedback on bank angle, the wings level indication signal. The DLEF device was chosen to prevent yaw moment coupling since it does not contribute to the yaw moment coefficient as shown in Table 2. A positive feedback gain $G_{DLEF/\varphi}$ was applied to effect a restoring moment to return the bank angle φ to level flight. Secondly, roll rate feedback was used to enhance the roll and yaw damping. The usual method of damping the Dutch roll is to detect the yaw rate with a rate gyro and use this signal to deflect a rudder. The ICE configuration has no rudder so the approach taken here was to add yaw damping through the yaw moment control on the DAMT device. This was the only device of the four considered which produces yaw moment. The final gains selected for the control system are shown below.

$$DAMT = 120p + 60r + 20\varphi$$
$$DLEF = 50p - 400r + 20\varphi$$

Here, there is no requirement for a side slip measurement but, as previously mentioned, this solution may not be satisfactory near the ground. The gains are in radian measure so that a one degree of bank angle signal produces a quasi-static shape change command of three-tenths on the port side AMT, meaning that, assuming linearity, the surface distortion required and commanded is approximately one-third the size shown in Figure 5. The starboard command is zero.

8. AUGMENTED AIRCRAFT DYNAMICS

Simulated aircraft responses with a wings leveler autopilot are shown in Figure 8. The responses are the result of a 1 degree initial condition in bank angle. Comparison with Figure 7 shows that the wings level function is indeed fulfilled since the simulated aircraft returns to zero angle of bank in approximately 11 seconds. The autopilot corrects the bank angle error with angular rates that are all small and side slip excursions that are less than a tenth of one degree.

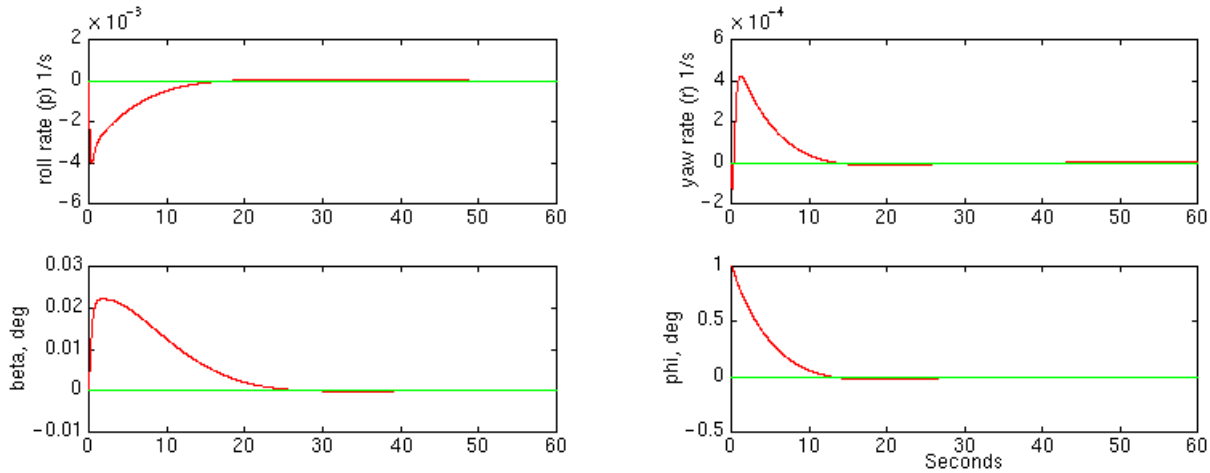

Figure 8 - Simulated responses of the aircraft with the wings leveler autopilot for a one degree initial condition on bank angle.

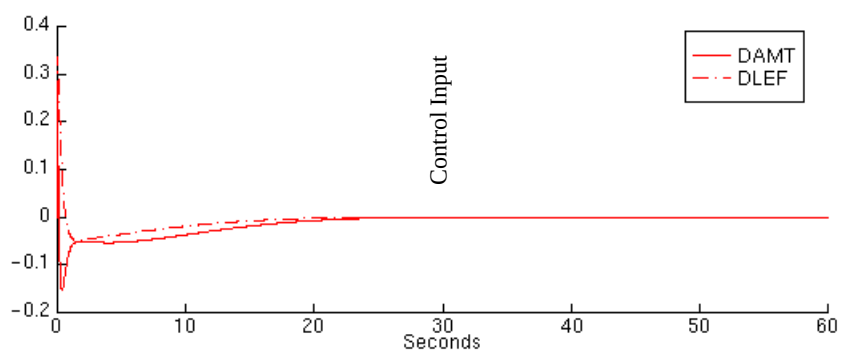

Figure 9 - Quasi-static shape change commands required for the simulation of Figure 8.

The quasi-static shape change commands (Figure 9) required are also small, starting at approximately 1/3 of the nominal LEF device shown in Figure 5 and reducing thereafter. The AMT has a maximum demand of about 1/5 the AMT surface change depicted in Figure 5, while maintaining the same geometric shape.

Although simulation in turbulence has not been conducted, relevant characteristics can be predicted by examining responses with initial conditions in side slip in addition to those of the angle of bank. This is shown in Figure 10. To correct for the one degree side slip, the aircraft banks with adverse yaw three degrees, port side down, and then returns to wings level. The side slip response is dead beat with no oscillations apparent.

The quasi-static shape change commands required for the simulation of Figure 10 are shown in Figure 11. The DLEF command is approximately twice the distortion shown in Figure 5 and the command of the AMT is about three and a half times that in Figure 5 (while maintaining the same geometric shape). Higher disturbances, up to 5 degrees side slip, demonstrated similar stability results, but required an order of magnitude increase in the magnitude of the quasi-static shape change shown in Figure 5.

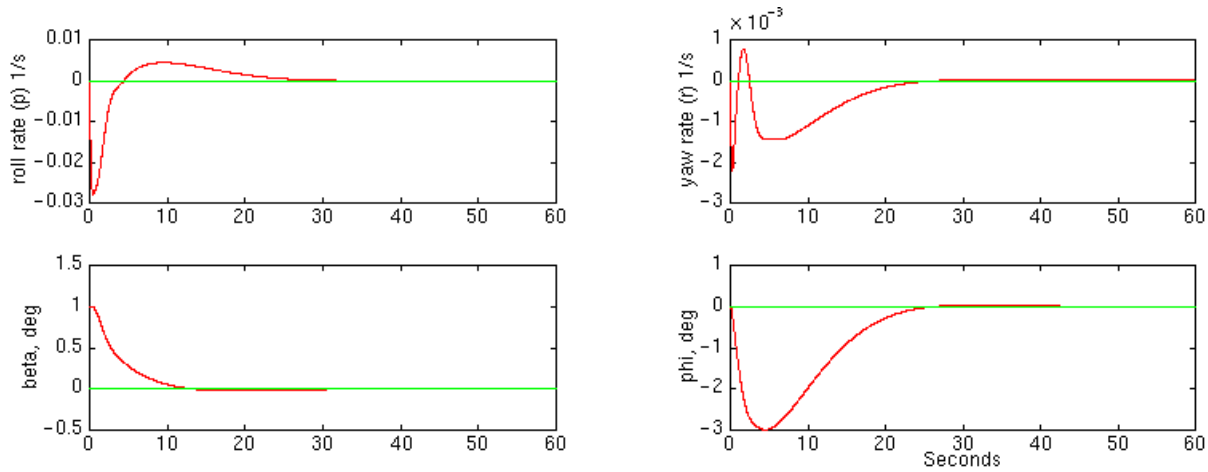

Figure 10 - Simulated responses of the aircraft with the wings leveler autopilot for a one degree side slip initial condition.

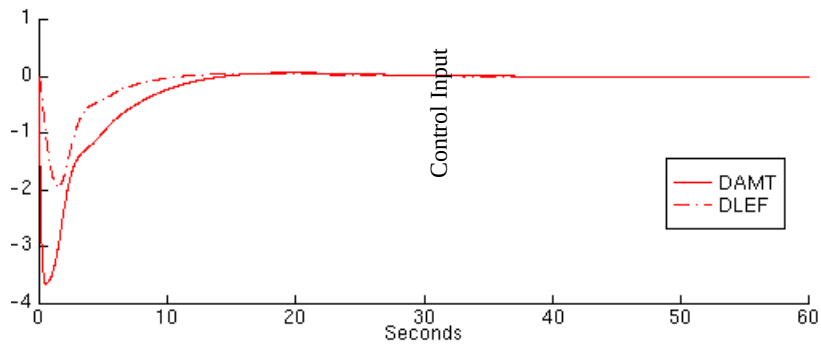

Figure 11 - Quasi-static shape change commands required for the simulation of Figure 10.

Because these are greater than the distortions input to the PMARC program, linearity cannot be assumed and whether or not the moments required can be produced must be verified with additional CFD runs. If pulsed jets are used to create the quasi-static shape change, viscous and boundary layer energizing would provide additional effects, i.e. reduced drag, increased lift, etc. In addition, optimal shape and location of the quasi-static shape change distortions will further improve the capability to stabilize larger initial transients and correct for side slip excursions.

9. CONCLUSIONS AND SUGGESTIONS FOR FUTURE RESEARCH

This paper represents an initial study of an ongoing effort to examine the effectiveness of quasi-static shape change distortions in the maneuvering of aircraft. The effector devices which create the surface distortions may be SMA (Shape Memory Alloys), piezoelectrics, pulsed jets, etc. The macroscopic effects of these devices are the focus of this study. Groups of devices are postulated to replace the conventional leading-edge flap (LEF) and the all-moving wing tip (AMT) devices on the tailless LMTAS-ICE (Lockheed Martin Tactical Aircraft Systems - Innovative Control Effectors) configuration. The maximum distortions were 13.8% and 7.7% of the section thickness for the design model LEF and AMT devices, respectively. A Computational Fluid Dynamics (CFD) panel code, PMARC, is used to determine the control effectiveness of groups of these devices. A preliminary design of a wings-leveler autopilot is also presented. Initial evaluation at 0.6 Mach at 15,000 ft. altitude is made through batch simulation. Results show small disturbance stability is achieved, however, an increase in maximum distortion is needed to statically offset five degrees of sideslip. This only applies to the specific device groups studied, encouraging future research on optimal device placement.

Future work is directed on two major fronts from the controls perspective, macroscopic controls and microscopic controls. In the macroscopic controls area, an ADIFOR (Automatic Differentiation of FORTRAN) tool will be utilized on CFD codes to determine the optimal groupings and locations of the quasi-static shape change devices. Given a FORTRAN source code and a specification of dependent and independent variables, ADIFOR generates an augmented derivative code that computes the partial derivatives of all the dependent variables with respect to all of the independent variables in addition to the original code. ADIFOR has been used successfully on a variety of codes of up to hundreds of thousands of lines in length. When a

CFD code is differentiated with respect to the far field boundary conditions, the stability and control derivatives are produced directly, which will expedite the control development process. This will significantly improve the generation of mathematical models used in active feedback flight controls for Morphing aircraft systems. In addition, the same ADIFOR process will be applied to the near field boundary conditions. This will provide sensitivity derivatives which will aide optimal effector placement design.

In the microscopic controls area, future studies will involve microscopic physics of these devices. Modeling the effluent on steady-jets would provide higher accuracy. Accuracy would also be improved by using higher fidelity CFD codes such as Navier Stokes simulations. More experimental work on these devices will also be used to validate simulation tools.

10. ACKNOWLEDGMENTS

The technical discussions with Dale Ashby at NASA Ames Research Center regarding the use and further development of the PMARC flow solver tool is gratefully appreciated. We would also like to thank Norma Bean of Computer Sciences Corporation for her adept work in modifying the geometry files to produce the surface distortions in this report. The authors would also like to thank Linda Kral for the fruitful technical discussions regarding the Navier Stokes modeling of steady jets.

11. REFERENCES

1. Active Structures Technical Committee: Abstracts of the Enabling Technologies for Smart Aircraft Systems Workshop, Internet document, http://afcmac.larc.nasa.gov/, March 14-16, 1996.
2. A. Pisano, Micro Electro Mechanical Systems (MEMS) at DARPA. Summer, 1997. Internet document, http://web-ext2.darpa.mil/ETO/MEMS/MEMS-OV.
3. A. Seifert, A. Darabi, and I. Wygnanski "Delay of Airfoil Stall by Periodic Excitation," *Journal of Aircraft*, Vol. 32, No. 4, July - August 1996.
4. K. M. Dorsett and D.R. Mehl, "Innovative Control Effectors (ICE)," Wright Laboratory Report, WL-TR-96-3043, January 1996.
5. L. Prandtl, and O. G. Tietjens: *Fundamentals of Hydro- and Aeromechanics*, Dover Publications, Inc., New York, 1957.
6. J. Katz and A. Plotkin, *Low-Speed Aerodynamics - from Wing Theory to Panel Methods*, McGraw-Hill, Inc. New York.
7. D.L. Ashby, M. R. Dudley, and S. K. Iguchi, "Development and Validation of an Advanced Low-Order Panel Method," NASA TM 101024, Oct. 1988.
8. J.F. Donovan, L.D. Kral, and A.W. Cary, "Active Flow Control Applied to an Airfoil," 36th AIAA Aerospace Sciences Meeting, paper AIAA 98-0210, Jan. 1998.
9. G. H. Bryan, *Stability in Aviation*, Macmillan Co., London, 1911.
10. B. Etkin, *Dynamics of Flight - Stability and Control*, John Wiley and Sons, Inc., New York, 1959.
11. J.H. Blakelock, *Automatic Control of Aircraft and Missiles*, John Wiley and Sons, Inc., New York, 1965.